Supporting Information for "Formation of tropical anvil clouds by slow evaporation"

Jacob T. Seeley[1], Nadir Jeevanjee[2,3], Wolfgang Langhans[4], and David M. Romps[1,4]

Contents of this file

1. Text S1 to S5

2. Figures S1 to S11

---

[1]Department of Earth and Planetary Science, University of California (Berkeley), Berkeley, CA 94720

[2]Department of Geosciences, Princeton University, Princeton, NJ 08544

[3]Geophysical Fluid Dynamics Laboratory, Princeton, NJ 08540

[4]Climate and Ecosystem Sciences Division, Lawrence Berkeley National Laboratory, Berkeley, CA 94720

Supplementary Figures

1. Figure S1
2. Figure S2
3. Figure S3
4. Figure S4
5. Figure S5

Text S1: Cloud-resolving model experiments The cloud-resolving model (CRM) used in this study is DAM, a three-dimensional, fully-compressible, nonhydrostatic CRM (Romps, 2008). All simulations were conducted on a square domain with a side length of 64 km and doubly periodic horizontal boundaries. Horizontal-mean winds were damped to zero on a time scale of six hours. The SST was fixed at 300 K for all simulations and surface fluxes were computed via a standard bulk aerodynamic formula.

In all simulations, cloudy grid cells were identified as those in which $q_c \geq 10^{-5}$ kg/kg, where q_c is the mass fraction of non-precipitating cloud condensate. We further divide cloudy air into "updraft" and "inactive" categories with a vertical velocity threshold: cloudy updrafts have $w \geq w_0(z)$, while inactive cloudy air has $w < w_0(z)$. The threshold w_0 ramps up linearly in altitude from 10^{-5} m/s at an altitude of 500 m to a constant of 2 m/s at altitudes above 3 km.

For the DEFAULT and DEFAULT_CLR simulations, the horizontal resolution was 200 m, and the vertical grid spacing increased from 50 m in the boundary layer to a constant 100 m spacing for altitudes between 2 km and 16 km, and increased again to 1 km between 24 km and the model top at 30 km. The time step was 5 s, which was sub-stepped to satisfy

a CFL condition. These simulations were restarted from equilibrated lower-resolution simulations and run to statistical equilibrium, after which statistics were collected over 10 days of model time. All figures in this manuscript based on these experiments are made from data that were averaged over this equilibrated 10-day period.

The microphysics scheme for these simulations was DAM's default six-class Lin-Lord-Krueger scheme (Krueger, Fu, Liou, & Chin, 1995; Lin, Farley, & Orville, 1983; Lord, Willoughby, & Piotrowicz, 1984). The Lin-Lord-Krueger scheme includes parameterizations for 28 different ice- and liquid-water microphysical processes.

These simulations were forced by radiative transfer as computed by RRTM (Clough et al., 2005; Iacono et al., 2008), using a trace gas profile with no ozone and a constant volume mixing ratio of 280 ppmv CO_2. For DEFAULT, the effect of cloud liquid and ice condensate on radiative transfer was included, while for DEFAULT_CLR, these effects were removed.

For the CTRL, NOEVAP, NOPEAK, and LOPEAK experiments, the horizontal resolution was 2 km, and the vertical grid spacing increased from 50 m in the boundary layer to a constant 250 m spacing for altitudes between 2 km and 16 km, and increased again to 1 km between 22 km and the model top at 30 km. The time step was 20 s, which was sub-stepped to satisfy a CFL condition. The CTRL experiment was forced by clear-sky radiative transfer computed by RRTM, while the NOEVAP, NOPEAK, and LOPEAK experiments were forced by prescribed radiative cooling profiles described in more detail below. These simulations were run to statistical equilibrium, after which statistics

were collected over 25 days of model time. All figures in this manuscript based on these experiments are made from data that were averaged over this equilibrated 25-day period.

For these four experiments, microphysics was treated with a simple Kessler-type scheme (Kessler, 1969) in order to facilitate a quantitative analysis of cloud sinks. There is no explicit ice phase in this scheme, so the only classes of water are vapor (with mass fraction q_v), non-precipitating cloud condensate (q_c), and precipitation (q_p). Other than the condensation and evaporation that occur during saturation adjustment, the only microphysical process included in this scheme is autoconversion of cloud condensate to precipitation, which was parameterized as

$$a = -q_c/\tau_a, \tag{1}$$

where a (s^{-1}) is the sink of cloud condensate from autoconversion and τ_a (s) is an autoconversion timescale that we discuss in more detail below. Precipitation is given a fixed freefall speed of 10 m/s and is allowed to evaporate in subsaturated air.

In inactive air, we set $\tau_a = 75$ minutes. In cloudy updrafts, τ_a was varied with height in order to approximately emulate the updraft-mean condensate loading from the DEFAULT simulation, which uses DAM's default six-class Lin-Lord-Krueger scheme (Krueger et al., 1995; Lin et al., 1983; Lord et al., 1984). By trial and error, we found that a reasonable match is achieved with a τ_a that ramps down from 30 minutes at and below an altitude of 500 m to a constant of 3.5 minutes at altitudes above 3 km. Figure S2 shows that the cloud fraction, updraft-mean cloud condensate loading, and precipitation flux from CTRL are similar to those from DEFAULT.

The subsections below detail further aspects of the CRM configuration in the NOEVAP, NOPEAK, and LOPEAK experiments.

NOEVAP experiment

The NOEVAP experiment was designed to be as similar to the CTRL experiment as possible except for the fact that cloud condensate was not allowed to evaporate in NOEVAP. Evaporation of cloud condensate was prevented in this experiment by intervening in the saturation-adjustment step of the CRM integration. Ordinarily, the job of the saturation adjustment routine is to move water between the vapor phase and condensed phases to ensure that grid cells are neither supersaturated, nor subsaturated in the presence of condensed water. Supersaturations are eliminated by moving vapor to the condensed phases; subsaturations in the presence of condensed water are corrected by evaporating/sublimating the condensed phase until the grid cell is either saturated or devoid of condensed water. The outputs of this saturation adjustment routine are tendencies of water vapor q_v and non-precipitating cloud condensate q_c, which (in a standard simulation) are then used as source terms in the governing equations for the water species in the model.

In NOEVAP, the saturation adjustment routine is initially called at each time step as usual. But, if the output of the saturation adjustment routine calls for evaporation of non-precipitating cloud condensate, those tendencies are not passed to the governing equations for water. If the saturation adjustment routine calls for condensation, everything proceeds as normal. In this way, cloud condensate is allowed to form but is prevented from evapo-

rating in the NOEVAP experiment. Note that precipitation is still allowed to evaporate in this experiment.

Preventing the evaporation of cloud condensate has two obvious effects on the atmosphere: 1) it reduces the mean relative humidity, because evaporation of detrained cloud condensates is an important source of water vapor in the free troposphere; and 2) it reduces the evaporative cooling in clear air, thereby reducing the amount of gross convective heating that is required to balance the sum of radiative and evaporative cooling in steady-state RCE. Since our intention with the NOEVAP experiment is to turn off cloud evaporation but keep everything else the same, it is desirable to correct for these two knock-on effects.

Therefore, the environmental relative humidity (RH) in NOEVAP was nudged toward the RH profile from CTRL on a timescale of $\tau_{\rm RH} = 15$ minutes. The results of this experiment are not sensitive to the value of $\tau_{\rm RH}$ for $\tau_{\rm RH} \leq 1$ hour. This nudging was only applied to non-cloudy grid cells in order to avoid interfering with the cloud decay process, and was enacted by a forcing term in the governing equation for water vapor F_{q_v} of the form

$$F_{q_v} = \rho \frac{{\rm RH}^\dagger q_v^* - q_v}{\tau_{\rm RH}}, \tag{2}$$

where ${\rm RH}^\dagger$ is the target RH from the CTRL experiment and q_v^* is the saturation specific humidity.

The main concern with the reduced evaporative cooling in NOEVAP is that there would be less convective mass flux and, consequently, less cloudy-air detrainment than in the CTRL experiment. Since our goal with this experiment is to change the sink of cloud con-

densate without changing the source, we modified the radiative cooling profile in the NOEVAP experiment until the volumetric detrainment rate in the free troposphere matched that from CTRL. Figure S6 shows that these forcings produced a close match between the RH and volumetric-detrainment profiles in the CTRL and NOEVAP experiments.

NOPEAK and LOWPEAK experiments

Here we describe our technique for producing a cloud-resolving RCE simulation with a desired profile of clear-sky convergence (as in the NOPEAK and LOPEAK experiments). The basic idea of our forcing scheme is to modify the radiative cooling rate until a desired convective mass flux profile is obtained. Let $M^\dagger$ be the desired mass flux profile, and let M_i be the measured mass flux from our simulation, averaged over a period with index i of duration Δt. Likewise, Q_i is the measured radiative cooling rate averaged over period i. The fractional error in the mass flux profile over period i is $f_i = (M^\dagger - M_i)/M^\dagger$. This error is then used as a correction to the radiative cooling rate $Q_{i+1} = Q_i(1 + f_i)$. This corrected cooling rate will produce a new profile of convective mass flux during period $(i+1)$, which will again be compared to the desired profile and used to produce a further correction to the cooling rate to be used during period $(i+2)$, and so on, until the cooling profile converges and a quasi-steady state is reached. We use an averaging window of $\Delta t = 6$ days, which sensitivity tests showed was sufficiently long for convective mass flux to equilibrate appropriately to the updated radiative cooling profiles.

At altitudes below 900 m (i.e., in the vicinity of the dry-convective boundary layer), we simply apply a vertically-uniform cooling rate of -0.011 (-0.015) W/m^3 in the NOPEAK (LOPEAK) experiments. Since there is no net radiative cooling (or convective mass flux)

in the stratosphere, at altitudes above 18.5 km we simply relax the temperatures to their domain-mean values from the CTRL simulation on a timescale of 6 hours. Finally, since the NOPEAK and LOPEAK simulations have, respectively, roughly 1.5 and 1.75 times as much tropospherically-integrated radiative cooling as the CTRL simulation, the bulk surface fluxes are uniformly scaled up by these factors in these two experiments. This serves to keep all three experiments on moist lapse rates rooted to a common near-surface air temperature of 298.5 $\pm$ 0.25 K. Our results do not depend on this modification of the surface fluxes. Figure S7 shows the steady-state radiative cooling and cloudy updraft mass flux profiles from the CTRL, NOPEAK, and LOPEAK experiments.

Text S2: Analytical cloud decay model Consider a cylindrical cloud with initial radius r_0 and constant height h. We assume the cloud is initially filled with turbulence with a uniform eddy velocity of v_0, so that the cloud's total kinetic energy is

$$\mathrm{KE} = \pi r_0^2 h \left(\frac{1}{2} \rho v_0^2 \right). \tag{3}$$

We further assume that the cloud's boundary expands radially outward at a rate proportional to the cloud's internal eddy velocity v:

$$\frac{dr}{dt} = cv, \tag{4}$$

where c is a dimensionless constant. For a quiescent environment and in the limit of no dissipation, the cloud conserves its kinetic energy as it grows, which implies that the product rv is constant in time. From equation 3, this constant is

$$rv = r_0 v_0 = \sqrt{\frac{2\mathrm{KE}}{\pi \rho h}}. \tag{5}$$

Combining equations 4 and 5, we find

$$\frac{d}{dt}\left(r^2\right) = 2cr_0v_0. \tag{6}$$

Therefore, the cloud's area A grows linearly in time:

$$A(t) = \pi r_0^2 + 2\pi r_0 c v_0 t = A_0\left(1 + t/\kappa\right), \tag{7}$$

where $A_0 = \pi r_0^2$ is the cloud's initial area and $\kappa \equiv r_0/(2cv_0)$ is a constant with dimensions of time. κ can be interpreted as the amount of time it takes the cloud to grow in area by an amount equal to its initial area A_0. We treat κ as a tuning parameter, which was optimized by a procedure described below.

To determine the lifetime of the cloud, we consider its bulk water budget (i.e., the cloud's properties are assumed to be homogeneous). Initially, the cloud has total water mass fraction $q_t = q_{c0} + q_v^*$, so that its total water mass is $M_t = Mq_t$, where the cloud's mass is $M = \rho hA$. The cloud's environment has total water $q_e = \mathrm{RH}q_v^*$, where RH is the environmental relative humidity. The cloud gains water as it grows, at the rate

$$\frac{dM_t}{dt} = \frac{dM}{dt}q_e = \left(\frac{\rho h A_0}{\kappa}\right)\mathrm{RH}q_v^*. \tag{8}$$

Therefore, the cloud's q_t evolves in time according to

$$\frac{dq_t}{dt} = -\left(\frac{1}{\kappa + t}\right)\left[q_c(t) + q_v^*(1 - \mathrm{RH})\right]. \tag{9}$$

As long as the cloud is saturated, its vapor mass fraction q_v is pegged at the saturation value q_v^* (which we take to be constant in time, neglecting changes in cloud temperature during the decay process.) Therefore, equation 9 is really the governing equation for the cloud's condensed water q_c. The solution is

$$q_c(t) = \frac{\kappa q_{c0} - q_v^*(1 - \mathrm{RH})t}{\kappa + t}. \tag{10}$$

Since we define cloudy air as having $q_c \geq 10^{-5}$ kg/kg, we can use equation 10 to solve for the mixing-only lifetime of the cloud, $\tilde{\tau}_{\text{mix}}$:

$$\tilde{\tau}_{\text{mix}} = \kappa \chi_c, \tag{11}$$

where

$$\chi_c \equiv \frac{q_{c0} - 10^{-5}}{q_v^*(1 - \text{RH}) + 10^{-5}}. \tag{12}$$

Note that the cloud grows as its mean cloud condensate is diminished, so that its maximum area occurs at the moment just before it "dies". From equation 7, the cloud's final area at time of death is

$$A(\tilde{\tau}_{\text{mix}}) = A_0 \left(1 + \chi_c\right). \tag{13}$$

So far, we have neglected an important sink of cloud condensate in decaying clouds: precipitation. If precipitation (parameterized by equation 1, in accordance with our simulations) were the only process causing clouds to decay, the governing equation for q_c would be

$$\frac{dq_c}{dt} = -q_c/\tau_a, \tag{14}$$

where τ_a is the autoconversion timescale. The solution is

$$q_c(t) = q_{c0} e^{-t/\tau_a}. \tag{15}$$

The lifetime is then

$$\tilde{\tau}_{\text{precip}} = \tau_a \log\left(q_{c0}/10^{-5}\right), \tag{16}$$

where the "precip" subscript indicates this is the effective lifetime for precipitation-only decay.

When both precipitation and mixing are included as sinks for cloud condensate, equation 9 is modified to

$$\frac{dq_t}{dt} = -\left(\frac{1}{\kappa + t}\right)\left[q_c(t) + q_v^*(1 - \mathrm{RH})\right] - q_c(t)/\tau_a, \tag{17}$$

where τ_a is the autoconversion timescale. The new solution is

$$q_c(t) = \frac{\kappa q_{c0} e^{-t/\tau_a} - q_v^*(1 - \mathrm{RH})\tau_a\left(1 - e^{-t/\tau_a}\right)}{\kappa + t}. \tag{18}$$

Setting equation 18 equal to 10^{-5} and solving for t yields the new expression for the cloud's lifetime $\tilde{\tau}$:

$$\tilde{\tau}_{\mathrm{new}} = \tau_a\left[W\left(ae^b\right) - b\right], \tag{19}$$

where

$$a = \frac{\kappa}{\tau_a}\left(\frac{q_{c0}}{10^{-5}}\right) + \frac{q_v^*(1 - \mathrm{RH})}{10^{-5}}, \tag{20}$$

$$b = \frac{\kappa}{\tau_a} + \frac{q_v^*(1 - \mathrm{RH})}{10^{-5}}, \tag{21}$$

and where W is the Lambert W function. Since W is defined by $W(xe^x) = x$, it is easy to verify from equation 19 that $\tilde{\tau} = 0$ when $q_{c0} = 10^{-5}$.

For time-mean cloud fraction, what matters is the time-integrated area of the cloud. Therefore, it is convenient to define an "effective lifetime", τ, such that a cloud that has constant area of A_0 during a lifetime of length τ would produce the same time-integrated cloud fraction as one that grows for a lifetime of $\tilde{\tau}$ as it decays:

$$\tau = \int_0^{\tilde{\tau}} \frac{A(t)}{A_0}\, dt. \tag{22}$$

For mixing-only decay, the time-integrated area is

$$\int_0^{\tilde{\tau}_{\mathrm{mix}}} A(t)dt = A_0\kappa\left(\chi_c + \frac{\chi_c^2}{2}\right), \tag{23}$$

which means that the the effective lifetime is

$$\tau_{\text{mix}} = \kappa \left(\chi_c + \frac{\chi_c^2}{2} \right). \tag{24}$$

The effective lifetime for precipitation-only decay is already given by equation 16 since such a cloud decays in place. Finally, with mixing and precipitation combined, the cloud's time-integrated area is

$$\int_0^{\tilde{\tau}_{\text{new}}} A(t)dt = A_0 \tilde{\tau}_{\text{new}} + \left(\frac{A_0}{2\kappa} \right) \tilde{\tau}_{\text{new}}^2, \tag{25}$$

while its effective lifetime is

$$\tau_{\text{new}} = \tilde{\tau}_{\text{new}} + \frac{\tilde{\tau}_{\text{new}}^2}{2\kappa}. \tag{26}$$

To summarize, we have obtained the following expressions for effective cloud lifetimes:

$$\tau_{\text{precip}} = \tau_a \log \left(q_{c0}/10^{-5} \right), \tag{27}$$

$$\tau_{\text{mix}} = \kappa \left(\chi_c + \frac{\chi_c^2}{2} \right), \tag{28}$$

$$\tau_{\text{new}} = \tilde{\tau}_{\text{new}} + \frac{\tilde{\tau}_{\text{new}}^2}{2\kappa}, \tag{29}$$

where χ_c is defined in equation 12 and $\tilde{\tau}_{\text{new}}$ in equation 29 is given by equations 19–21.

Optimizing κ

In this analytical model of cloud decay, κ (units of seconds) appears as the single free parameter. κ characterizes the rate of turbulent cloud spreading: according to equation 7, κ is the amount of time it takes for a cloud to grow by an amount equal to its initial area A_0. Here we optimize the value of κ used in the analytical expression for cloud lifetimes, τ_{new}, for the CTRL, NOEVAP, NOPEAK, and LOPEAK experiments.

Let $\mathcal{C}_i(z)$ be the actual cloud-fraction profile (with updrafts removed) measured in the CRM from an experiment indexed by i, and let $\mathcal{C}_i^\dagger(z)$ be the cloud-fraction profile predicted for that experiment by the new framework with a particular value of κ (i.e., predicted by equation 14 from the main text, with τ_{new} given by equation 29). We define the following cost function

$$\text{cost function} = \sum_{i=1}^{3} \frac{1}{z_{\text{top}}} \int_0^{z_{\text{top}}} \left[\mathcal{C}_i(z) - \mathcal{C}_i^\dagger(z)\right]^2 \mathrm{d}z, \tag{30}$$

where $i = 1$ corresponds to the CTRL experiment, $i = 2$ to the NOPEAK experiment, and $i = 3$ to the LOPEAK experiment. We optimize the value of κ by minimizing this cost function.

Figure S8 shows the value of the cost function for κ in the range of 1–80 minutes. The cost function has a minimum at $\simeq$19 minutes, which we take to be the "best" value κ_{best} used throughout this manuscript. The minimum in the cost function is fairly broad — κ can be varied by a factor of 2 in either direction without much degradation of the fit, as can be seen in the bottom row of Figure S8. For larger values of κ (corresponding to increasingly slow turbulent mixing), predicted cloud lifetimes in the lower troposphere become unrealistically long, cloud fraction becomes too large, and the fit becomes worse.

Text S3: Numerical cloud decay model The analytical model of cloud decay presented in the previous section uses a bulk water budget, which means that mixing occurring at the edge of the cloud is instantaneously distributed throughout the entire cloud volume. Here we present a second model of decaying clouds that does not make this bulk assumption. Instead, we numerically solve the diffusion equation.

We assume that our decaying cloud consists of a radially-symmetric distribution of water vapor $q_v(r,t)$ and cloud condensate $q_c(r,t)$. The cloud begins life when it is detrained as a saturated top-hat with initial radius r_0 and condensate mass fraction q_{c_0}:

$$q_c(r,0) = \begin{cases} q_{c_0}, & \text{if } r \leq r_0 \\ 0, & \text{if } r > r_0 \end{cases} \tag{31}$$

$$q_v(r,0) = \begin{cases} q_v^*, & \text{if } r \leq r_0 \\ \text{RH} q_v^*, & \text{if } r > r_0 \end{cases} \tag{32}$$

where RH is the environmental relative humidity at the detrainment level.

The governing equations for q_v and q_c take the form of the radial diffusion equation with sources and sinks that account for the processes of saturation adjustment and precipitation:

$$\partial_t q_v = k\left[\partial_r^2 q_v' + \frac{1}{r}\partial_r q_v'\right] + e(r,t) \quad ; \tag{33}$$

$$\partial_t q_c = k\left[\partial_r^2 q_c + \frac{1}{r}\partial_r q_c\right] - e(r,t) - p(r,t) \quad , \tag{34}$$

where k (m^2/s) is the turbulent diffusivity, $e(r,t)$ (1/s) is the evaporation rate, and $p(r,t)$ (1/s) is rate at which cloud condensate is converted into precipitation.

Equations 33 and 34 are integrated numerically with an implicit Euler method. We discretize the radial coordinate r with 1000 points of size $\Delta r = 100$ m, and discretize the time coordinate with steps of length $\Delta t = 20$ s. The integration method is as follows. First, the distributions of q_v and q_c are diffused according to the radial diffusion operator acting alone. Second, a "saturation adjustment" step occurs, in which the evaporation is diagnosed as follows: at each grid point, condensed water is converted into vapor until $q_v = q_v^*$ or all q_c has evaporated. Third, cloud condensate is removed by precipitation, which is parameterized according to equation 1 in order to match the microphysics scheme

in the CRM experiments. At each time step, the radius of the cloud is the largest value of r at which $q_c(r,t) \geq 10^{-5}$. This procedure is repeated until the cloud's radius has shrunk to 0, at which point the cloud has reached its lifetime $\tilde{\tau}$ and is considered dead. As in the analytical cloud decay model, the effective lifetime of the cloud is diagnosed according to equation 22. This model of cloud decay has two free parameters: the initial radius r_0 and the diffusivity k.

Although the analytical and numerical cloud decay models differ in their details, they produce very similar results. In Figure S9, we show the effective cloud lifetimes predicted by the two models for the CTRL, NOEVAP, NOPEAK, and LOPEAK experiments. For the analytical model, the value of the free parameter κ is set to 19 minutes. For the numerical model, the diffusivity k is set to 500 m^2/s and the initial radius r_0 is set to 2 km. For the NOEVAP experiment, evaporation is prevented in the cloud decay models by setting $\mathrm{RH} = 1$.

In the CTRL, NOPEAK, and LOPEAK experiments, τ (as predicted by either the analytical or numerical models) has the characteristic top-heavy shape caused by inefficient evaporation in the upper troposphere (Figure S9). In the NOEVAP experiment, however, τ varies by only about a factor of 2 over the depth of the troposphere.

Text S4: Cloud fraction in RCE Here we derive an expression for steady-state cloud fraction in radiative-convective equilibrium. Consider a layer of an atmosphere in a square domain with side length L, observed during a time interval of length Δt, during which n clouds are born, grow, and die within that layer. Considered individually, each cloud

contributes a time-mean fractional area, C, given by

$$C = \frac{\int_0^{\tilde{\tau}} A(t)dt}{L^2 \Delta t}. \tag{35}$$

If the clouds have random overlap in space and time, the time-mean cloud fraction $\mathcal{C}(L^2\Delta t)$ during this interval is

$$\mathcal{C}(L^2\Delta t) = 1 - (1 - C)^n. \tag{36}$$

The number of clouds that form during this interval, n, is given by

$$n = \left(\frac{\delta M}{\rho}\right)\left(\frac{1}{A_0}\right) L^2 \Delta t. \tag{37}$$

The first term on the RHS of equation 37 is the volumetric detrainment rate, with M (kg/m^2/s) the convective mass flux and δ (1/m) the bulk-plume fractional detrainment rate.

To find the steady-state cloud fraction $\mathcal{C}$, we take the limit of equation 36 as $L^2\Delta t \to \infty$. This yields

$$\mathcal{C} = 1 - \exp\left[-\left(\frac{\delta M}{\rho}\right)\tau\right], \tag{38}$$

where we have recognized $\int_0^{\tilde{\tau}} (A/A_0)\, dt$ as the effective lifetime τ from equation 22. Taylor-expanding the exponential to first order yields

$$\mathcal{C} = \left(\frac{\delta M}{\rho}\right)\tau. \tag{39}$$

This is the result we would have obtained had we assumed no overlap between the clouds rather than random overlap. Note that equation 39 will make an unphysical prediction of $\mathcal{C} > 1$ in the limit of very large detrainment or very long cloud lifetimes; in such cases one should use equation 38 instead.

Identifying τ as τ_{new}, we obtain our equation for steady-state cloud fraction in RCE, valid in the limit of small cloud fraction (equation 14 in the main text). Note that equation 39 only accounts for the area occupied by decaying clouds, which overwhelmingly dominate cloud fraction above the boundary layer. For completeness, though, we can also include the area occupied by active convective mass flux $M/(\rho w)$, where w is the mean updraft velocity:

$$\mathcal{C} = \frac{M}{\rho}\left[\delta\tau + \frac{1}{w}\right]. \tag{40}$$

Text S5: Applying the new framework to the DEFAULT simulation The new framework for anvil clouds can, in principle, be applied to any CRM simulation, including DEFAULT. The challenge is that for DEFAULT, the precipitation timescale τ_a that enters into the expression for τ_{new} is an emergent property of the Lin-Lord-Krueger microphysics scheme — rather than a known parameter of the CRM, as it is for the simulations that use the simple microphysics scheme described in *Text S1*. This means that for DEFAULT there are now two unknown parameters entering into the new framework for anvil clouds: κ and τ_a, which control the rates of turbulent cloud spreading and precipitation, respectively. Therefore, we must perform a two-parameter optimization to find the best values for these timescales. As for our optimization of κ, we define the cost function

$$\text{cost function} = \frac{1}{z_{\text{top}}}\int_0^{z_{\text{top}}}\left[\mathcal{C}(z) - \mathcal{C}^\dagger(z)\right]^2 \mathrm{d}z, \tag{41}$$

where $\mathcal{C}(z)$ is the actual cloud-fraction profile from the DEFAULT experiment (with updrafts removed) and $\mathcal{C}^\dagger(z)$ is the cloud-fraction profile predicted by the new framework for a particular set of κ and τ_a values. Figure S10 shows the result of minimizing the cost function given by equation 41. The optimal values are $\kappa = 7.5$ minutes and $\tau_a = 43$

minutes. Note that this value of κ is about a factor of 2 smaller than the best-fit κ found for the lower-resolution simulations, which suggests that turbulent mixing is more efficient at finer horizontal resolution.

The right panel of Figure S10 shows that the new framework makes a very good prediction for the cloud-fraction profile of the DEFAULT simulation with these parameter values. This successful prediction requires using both the correct source term (the volumetric detrainment) and the correct cloud-lifetime profile (τ_{new}). If the CSC paradigm's source term (the clear-sky convergence) is used in conjunction with τ_{new}, the predicted cloud fraction has the correct top-heavy shape but is significantly too small in magnitude; on the other hand, if the correct source term (the volumetric detrainment) is used in conjunction with the CSC paradigm's constant-lifetime assumption, the predicted cloud-fraction profile is bottom-heavy, in stark contrast to the CRM results (Figure S11). Only when cloud fraction is predicted by the new framework is a good fit obtained.

References

Clough, S. A., Shephard, M. W., Mlawer, E. J., Delamere, J. S., Iacono, M. J., Cady-Pereira, K., ... Brown, P. D. (2005). Atmospheric radiative transfer modeling: A summary of the AER codes. *Journal of Quantitative Spectroscopy and Radiative Transfer*, *91*(2), 233–244. doi: 10.1016/j.jqsrt.2004.05.058

Iacono, M. J., Delamere, J. S., Mlawer, E. J., Shephard, M. W., Clough, S. A., & Collins, W. D. (2008). Radiative forcing by long-lived greenhouse gases: Calculations with the AER radiative transfer models. *Journal of Geophysical Research Atmospheres*, *113*(13), 2–9. doi: 10.1029/2008JD009944

Kessler, E. (1969). On the continuity and distribution of water substance in atmospheric circulations. *Atmospheric Research*, *38*(94), 109–145.

Krueger, S. K., Fu, Q., Liou, K. N., & Chin, H.-N. S. (1995). Improvements of an ice-phase mcrophysics parameterization for use in numerical simulations of tropical convection. *Journal of Applied Meteorology*, *34*(1).

Lin, Y.-L., Farley, R. D., & Orville, H. D. (1983). Bulk parameterization of the snow field in a cloud model. *Journal of Climate and Applied Meteorology*, *22*.

Lord, S. J., Willoughby, H. E., & Piotrowicz, J. M. (1984). *Role of a Parameterized Ice-Phase Microphysics in an Axisymmetric, Nonhydrostatic Tropical Cyclone Model* (Vol. 41). doi: 10.1175/1520-0469(1984)041¡2836:ROAPIP¿2.0.CO;2

Romps, D. M. (2008, dec). The Dry-Entropy Budget of a Moist Atmosphere. *Journal of the Atmospheric Sciences*, *65*(12), 3779–3799. doi: 10.1175/2008JAS2679.1

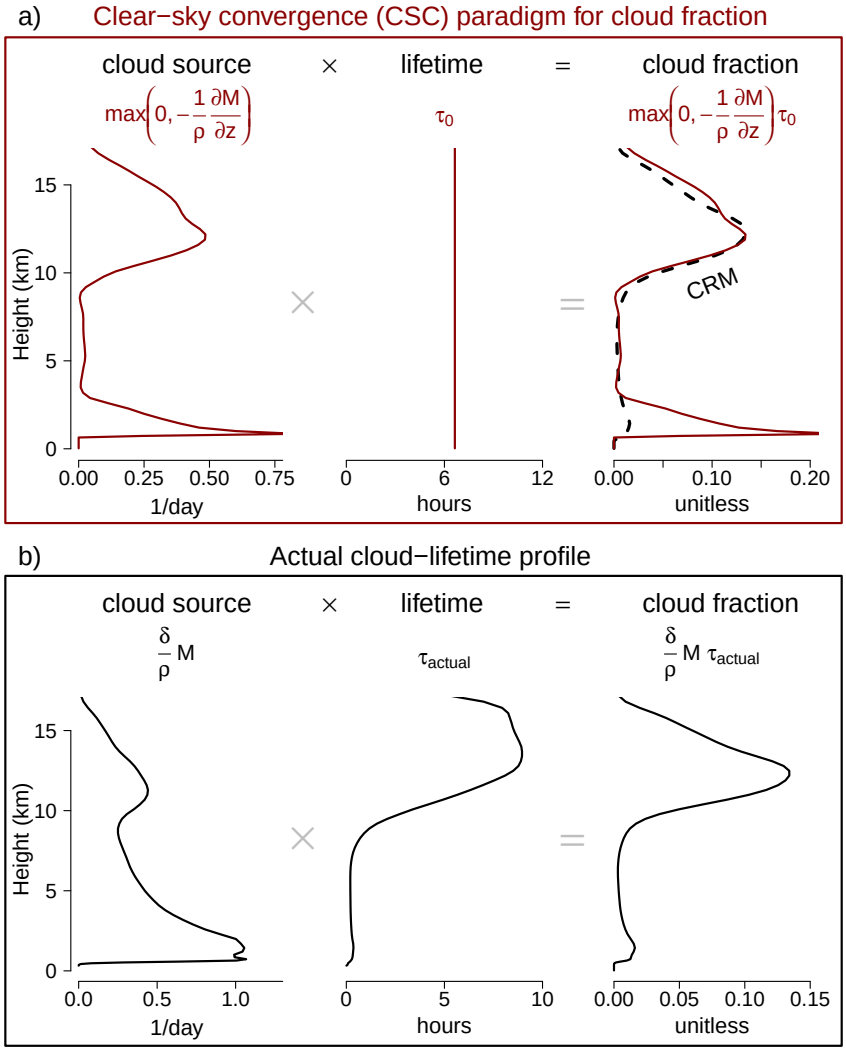

Figure 1. As in Figure 2 of the main text, but for the CTRL experiment rather than DEFAULT.

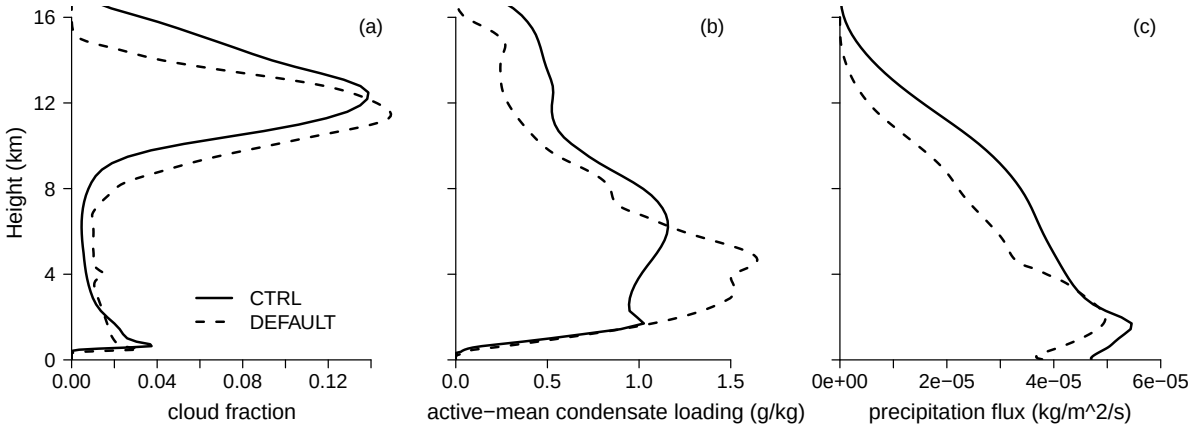

Figure 2. (a) Cloud fraction, (b) updraft-mean non-precipitating cloud condensate q_c, and (c) precipitation flux in the CTRL and DEFAULT simulations. For DEFAULT, q_c includes non-precipitating cloud liquid and cloud ice and the precipitation flux includes rain, snow, and graupel. For CTRL, neither q_c nor the precipitation flux are differentiated into liquid and ice subspecies because of the simple microphysics scheme used in that simulation.

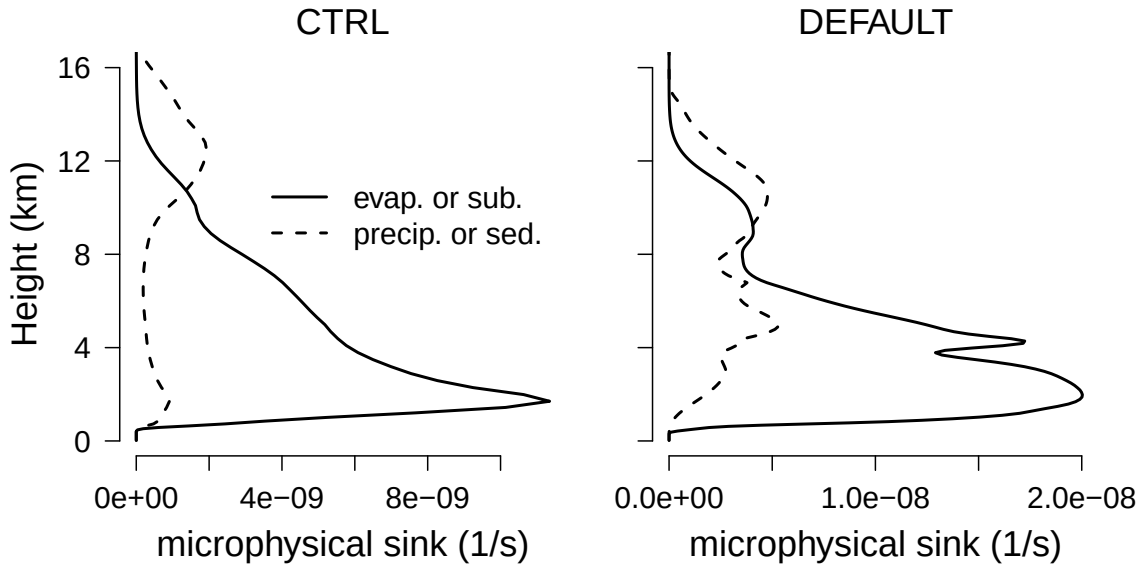

Figure 3. Microphysical sinks of non-precipitating cloud condensate, averaged in time and over inactive grid cells, for the (left) CTRL and (right) DEFAULT experiments. Solid lines show the sum of evaporation and sublimation, while dashed lines show the sum of precipitation and sedimentation (in the CTRL experiment, sublimation and sedimentation are both identically zero because of the simplified microphysics scheme in that simulation).

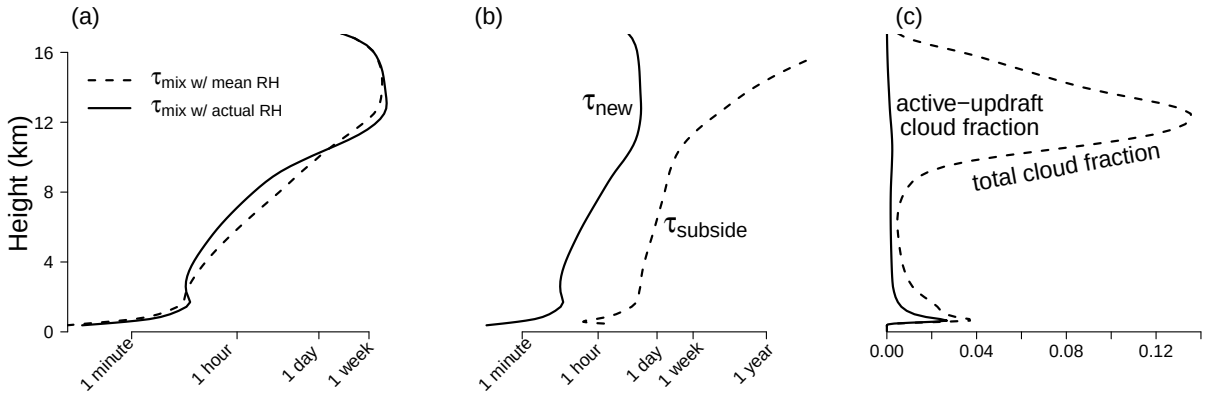

Figure 4. (a) From the CTRL experiment, the effective cloud lifetime from mixing-induced decay alone, $\tau_{\rm mix}$ (i.e., neglecting precipitation as a sink of cloud condensate; eqn. 24), both with the actual environmental RH from the simulation and with the mean tropospheric RH. (b) Effective cloud lifetime $\tau_{\rm new}$ compared to $\tau_{\rm subside}$. (c) Total cloud fraction from the CTRL experiment compared to the area occupied by updrafts alone.

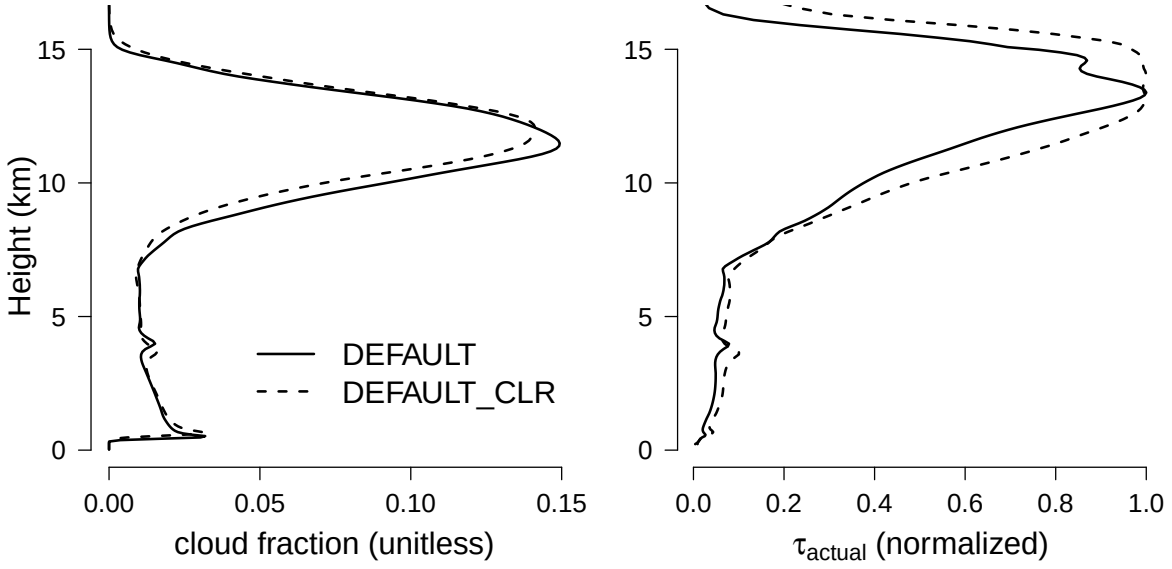

Figure 5. (left) Cloud fraction from the DEFAULT and DEFAULT_CLR simulations. In DEFAULT_CLR, cloud condensate is zeroed out in the radiative transfer calculations, rendering clouds invisible to radiation; the results show that the cloud-fraction profile is fairly insensitive to this change. (right) Diagnosed cloud-lifetime profiles (τ_{actual}) from the two simulations, normalized by their maximum values. As in Figure 2 of the main text, τ_{actual} is diagnosed by dividing the measured cloud fraction (with updrafts removed) by the measured volumetric detrainment. The similarly-shaped τ_{actual} profiles of the two experiments — in particular, the order-of-magnitude increase in cloud lifetimes in the upper troposphere shared by both profiles — shows that cloud-radiative interactions are not responsible for the ballooning of cloud lifetimes in the upper troposphere.

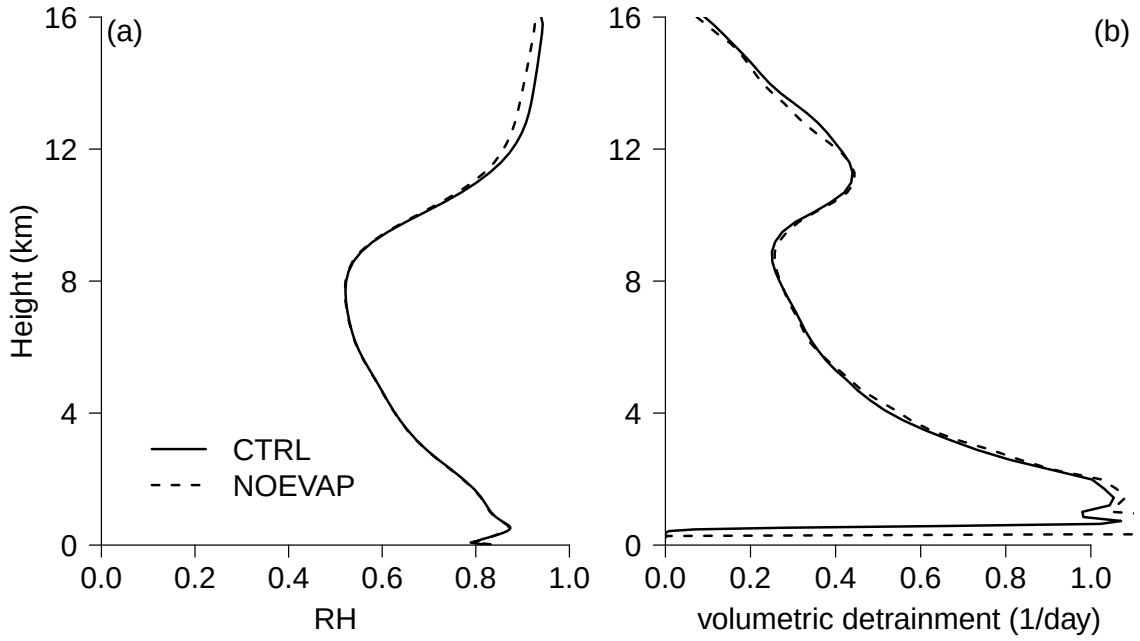

Figure 6. (a) Relative humidity, and (b) volumetric detrainment from the CTRL and NOEVAP experiments.

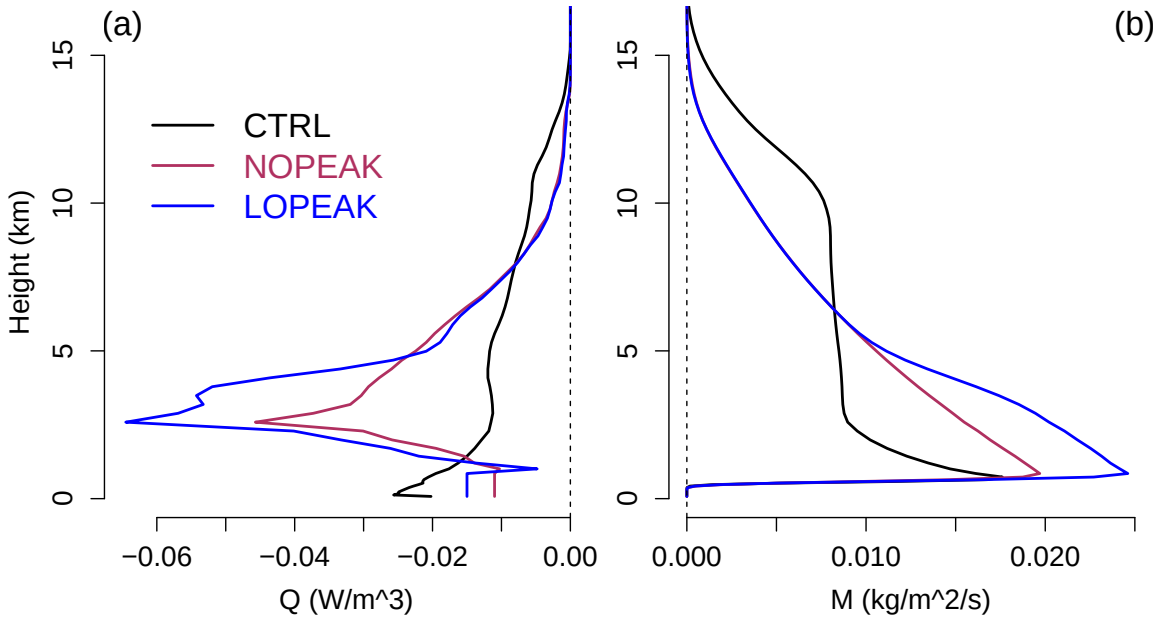

Figure 7. (a) Radiative cooling, and (b) cloudy updraft mass flux from the CTRL (black), NOPEAK (maroon), and LOPEAK (blue) experiments.

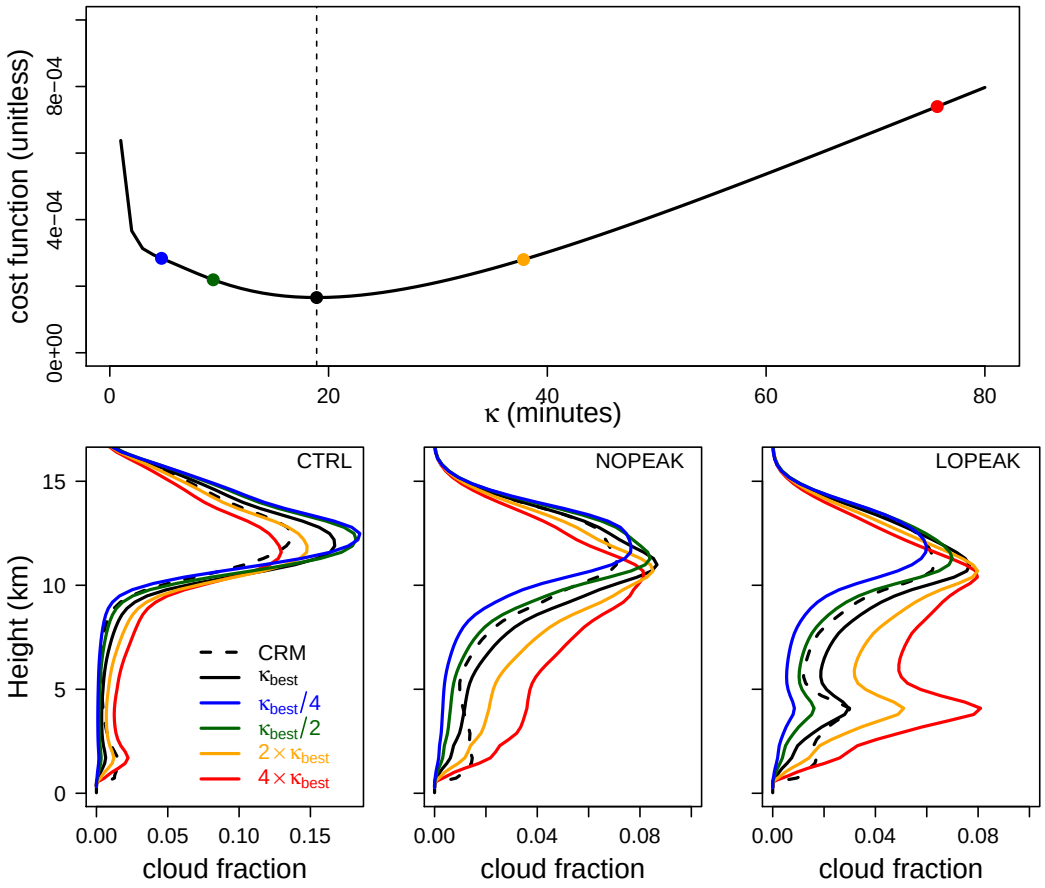

Figure 8. (Top panel) The value of the cost function given by equation 30 for κ in the range of 1–80 minutes. The black circle marks the minimum at $\kappa_{\rm best} = 19$ minutes, while the blue, green, orange, and red circles mark values of $\kappa_{\rm best}$ scaled by factors of 0.25, 0.5, 2, and 4, respectively. (Bottom row) The cloud-fraction profiles predicted by the new framework for the CTRL, NOPEAK, and LOPEAK experiments, for the values of κ shown in the top panel.

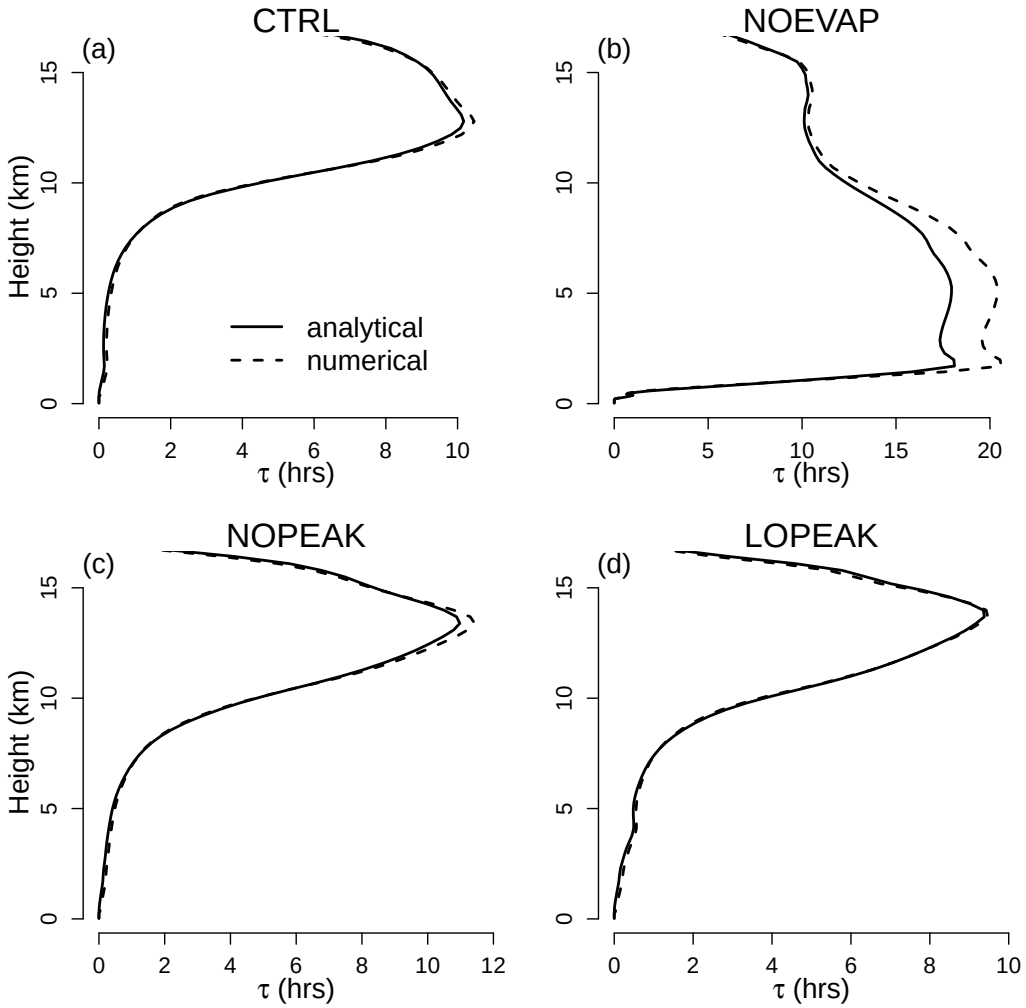

Figure 9. Effective cloud lifetimes predicted by the analytical and numerical models of cloud decay. Results are shown for four experiments: (a) CTRL, (b) NOEVAP, (c) NOPEAK, and (d) LOPEAK. For the analytical model, the free parameter κ is set to 19 minutes. For the numerical model, the turbulent diffusivity κ is set to 500 m^2/s, and the initial radius r_0 is set to 2 km.

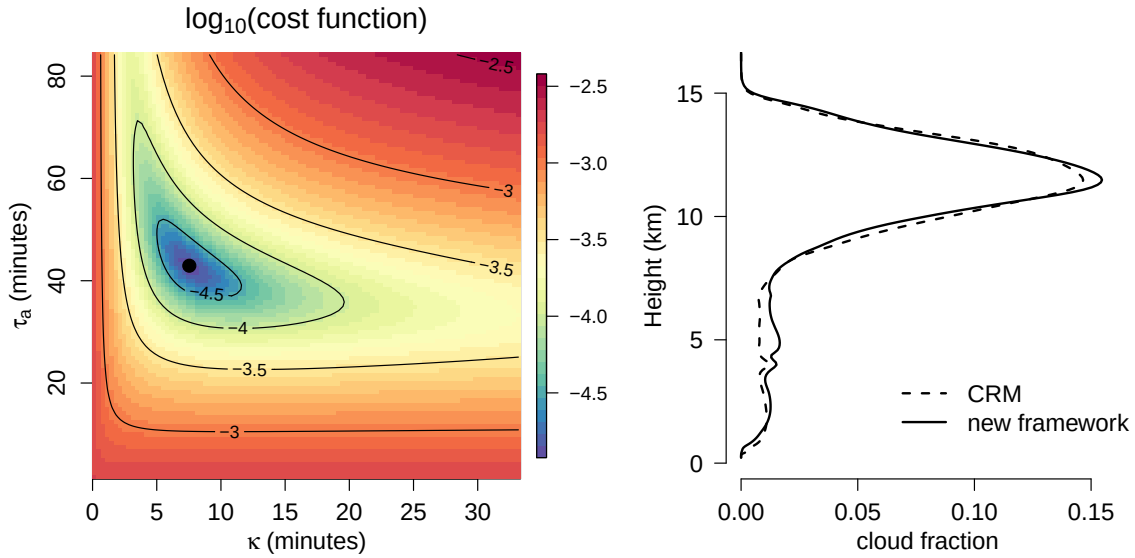

Figure 10. (left) The base-10 logarithm of the cost function given in equation 41, for a range of κ and τ_a values. The best-fit values ($\kappa = 7.5$ minutes and $\tau_a = 43$ minutes) are indicated with the filled black circle. (right) The cloud-fraction profile (with updrafts removed) from the DEFAULT simulation (dashed line), as compared to the cloud-fraction profile predicted by the new framework with the best-fit values of κ and τ_a (solid line).

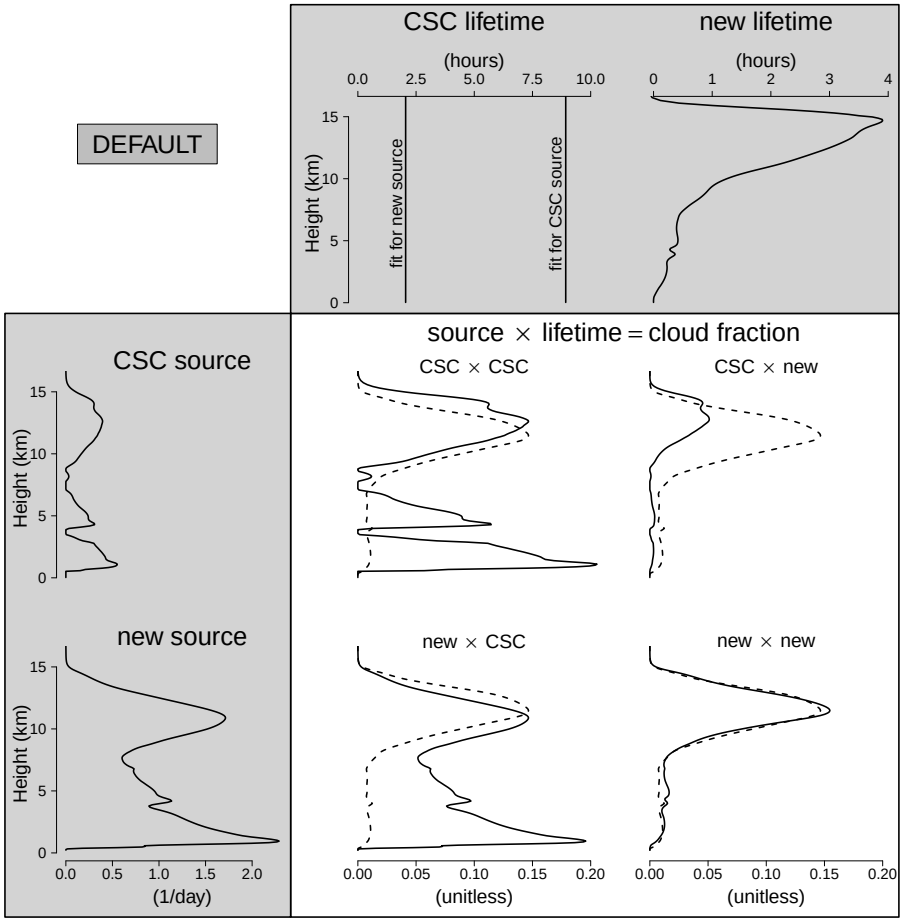

Figure 11. For the DEFAULT experiment: (top row) the cloud-lifetime profiles used by the CSC paradigm and the new framework (for the vertically-uniform cloud-lifetime profiles used by the CSC paradigm, separate values are fit for each of the two possible source terms); (first column) the cloud-source profiles used by the CSC paradigm and new framework; (four plots inside the black box) all possible products of these two sources and two lifetimes, which give four different predictions for the cloud-fraction profile. The actual cloud-fraction profile from the CRM is shown by the dashed line in the four plots inside the black box. Only when the new source (the volumetric detrainment, $\delta M/\rho$) is multiplied by the new cloud-lifetime profile (τ_{new}) is a good fit to the CRM obtained.